Published by :
http://www.ijert.org

International Journal of Engineering Research & Technology (IJERT)
ISSN: 2278-0181
Vol. 5 Issue 06, June-2016

Pipeline Blockage Detection

O. Srour
Graduate Student , ME,
Arab Academy for Science
Department of Mech. Eng.,
Alexandria , Egypt

E. Saber
Professor
Arab Academy for Science
Department of Mech. Eng.,
Alexandria , Egypt

H. A. Elgamal
Professor
Alexandria University
Department of Mech. Eng.,
Alexandria , Egypt

***Abstract*: A new technique is proposed for the detection of blockages in pipelines based on prediction of wall shear stress. Theoretical analysis for the flow in a pipe with blockage on part of its wall was considered where a small sinusoidal disturbance in flow is introduced artificially at pipe entrance to the original flow in order to have time changes in velocity distribution and wall shear stress capable of sensing the presence of blockage in the pipe. Numerical scheme is developed for solving the governing equations of motion using the finite difference method. Successive under relaxation method was used to solve the discretized equations. Results showed that there is a sudden increase in the shear stress at the beginning of blockage surface that decreases gradually till the end of the blockage. The shear stress at the blockage surface remains higher when compared to the wall shear stress in the non-blocked part of the pipe. From the resulting shear stress distribution, the location and length of blockage could be determined. The suggested model is capable of detecting blockage in pipeline no matter what the length of the blockage and its position in the pipeline are.**

Keywords: Pipeline; Blockage Detection; Shear Stress; Numerical Analysis.

I. INTRODUCTION

Pipeline is the most efficient way to convey fluids, where it is widely used in transportation of oil, natural gas, industrial plants networks and water distribution networks. Leaks and partial or complete blockages are common faults occurring in pipelines which causes problems. Leaks produce loss of fluid which leads to loss in pressure, production and economic cost, and in some cases it could affect the environment. Blockages impede flow leading to loss in pressure and hence increase the needed pumping force /cost to overcome the loss in pressure, and sometimes blockages could lead to complete stoppage of operation. Early detection and accurate location of leaks or blockages could help to avoid the problems caused by such faults and foster the right timing decision for dealing with such faults in order to avoid or minimize production/operation interruption.

Blockages could arise from condensation, solid depositions, or un-intentionally partially closed inline valves. Blockages are classified on the basis of their physical extent relative to the total length of the system. Localized constrictions that can be considered as point discontinuities are referred to as discrete blockages, while blockages that have significant length relative to total pipe length are termed extended blockages [1]

Unlike leaks within piping systems, a blockage does not generate clear external indicators for its location such as the release and accumulation of fluids around the pipe. Often intrusive procedures using instruments, such as the insertion of a closed-circuit camera or a robotic pig, are required to determine the location of blockages. Insertion of camera or robotic pig may have some uncertainties regarding the travelling speed and travelling distance between the insertion point and the blockage , where in many cases the camera or the robotic pig get stuck into the blockage and causes a bigger problem in this case than the presence of the blockage only. The creation of nonintrusive techniques for fault detection that gives a clear picture of the internal conditions of the pipeline is desirable [2], Non-destructive testing techniques as radiographic testing is commonly used as a non-intrusive test. Over the last two decades researchers have tried to develop flow analysis based techniques to detect blockages, methods that was developed used fluid transients depending on the response of the system to an injected transient for detecting, locating and sizing blockages; these non intrusive methods have shown a promising development.

The flow transients may be analyzed either in the time domain or in the frequency domain. In the time domain, the method of characteristics (MOC) is used to solve the governing partial differential equations [3], [4]. Two methods are available for analysis in the frequency domain: the impedance method [3] and the transfer matrix method [4] . [5]

Adewumi, Eltohami and Ahmed [6] , Adewumi, Eltohami and Solaja[7] proposed a time reflection method and conducted numerical experiments for detection of partial blockage of discrete and extended type in single pipeline for both single and multiple blockages. Vitovsky et al.[8] introduced an impulse response method for detection of leaks and partial blockages of discrete type in single pipeline and the method was tested numerically. Wang, Lambert and Simpson[9] utilized the damping of fluid transients based on analytical solution and experimental verifications for detection of partial single discrete blockage in single pipeline. Other researchers used Frequency Response Method for detection of discrete blockages type in single pipelines through numerical experiments [10], [11] and [2] and for detection of discrete blockages type in branched pipelines by [5]. Sattar, Chaudry and Kassem [11] compared the numerical results with laboratory experiments which showed that blockage location could be obtained with almost no error , while the size detection had some errors. Duan, Lee, Ghidaoui and Tung [1] proposed another technique based on Frequency Response Analysis for detection of single and multiple blockages of extended type in single pipeline, later Duan et al.[12] conducted analytical simplification to their previous work in

International Journal of Engineering Research & Technology (IJERT)
ISSN: 2278-0181
Vol. 5 Issue 06, June-2016

2012 and verified the numerical results through laboratory experiments. Meniconi et al. [13] proposed a coupled frequency and time – domain analysis for detection of single and multiple blockages of extended type in single pipeline, where the two methods were verified experimentally and the results showed that the time domain method (pressure signal analysis) is most accurate for locating the blockage and that the frequency domain method (frequency response analysis) is most accurate for determining the radial constriction and length of the blockage. Stephens, Lambert, Simpson, Vitkovsky and Nixon [14] and Stephens, Simpson and Lambert [15] conducted some field transient flow tests using time transient analysis to detect single discrete blockage in a single pipeline, the results showed good accuracy for detecting and locating blockage but with limitation that is for blockages with reduction in pipe cross section less than 67% the suggested model failed to detect the blockage. Bocchini, Marzani and Karamlou [16] proposed a technique to preliminary identify obstructed pipes in a pipe network relying on measurements that do not disrupt normal operation as head and flow measurements and to quantify the extent of each blockage (based on residual diameter) as a first phase and then to use one of the previously developed techniques by other researchers to locate blockage within the obstructed pipe. Wang et al. [17] proposed a technique for discrete blockage detection in gas pipelines utilizing the reflection of injected acoustic signal and the method was verified by field test.

II. THEORETICAL ANALYSIS

A. Governing Equations

For cylindrical polar coordinates and unsteady incompressible laminar flow in pipe, with no pressure driving conditions in the tangential direction, assuming axi-symmetric flow and assuming no flow swirl in θ – direction; the equations of motion for flow in the pipe with blockage (see **Fig. 1**) are given by:

$$\rho\left(\frac{\partial v_r}{\partial t}+v_r\frac{\partial v_r}{\partial r}+v_z\frac{\partial v_r}{\partial z}\right)=-\frac{\partial P}{\partial r}+\mu\left(\frac{\partial^2 v_r}{\partial r^2}+\frac{1}{r}\frac{\partial v_r}{\partial r}-\frac{v_r}{r^2}+\frac{\partial^2 v_r}{\partial z^2}\right) \quad (1)$$

$$\rho\left(\frac{\partial v_z}{\partial t}+v_r\frac{\partial v_z}{\partial r}+v_z\frac{\partial v_z}{\partial z}\right)=-\frac{\partial P}{\partial z}+\mu\left(\frac{\partial^2 v_z}{\partial r^2}+\frac{1}{r}\frac{\partial v_z}{\partial r}+\frac{\partial^2 v_z}{\partial z^2}\right) \quad (2)$$

And the continuity equation is given by:

$$\frac{\partial v_r}{\partial r}+\frac{v_r}{r}+\frac{\partial v_z}{\partial z}=0 \quad (3)$$

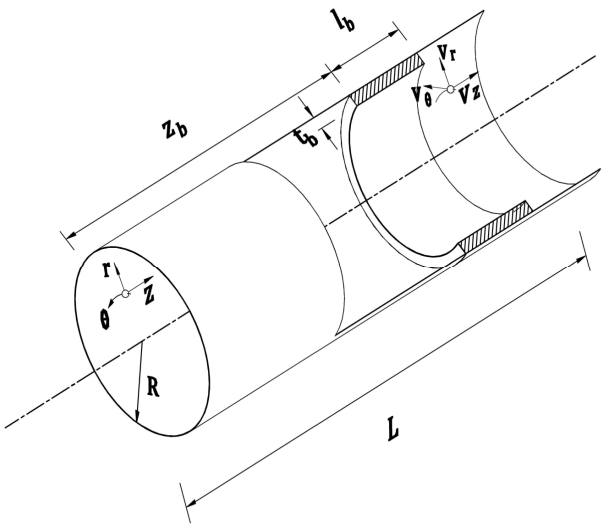

Fig. 1 : The pipe and blockage model used and the cylindrical polar coordinates system - sectioned for clarity

Where; r, θ and z are radial, angular and axial coordinates respectively and t is time. v_r ,v_θ , v_z and P are the velocity components in r, θ and z directions and the fluid pressure respectively. ρ and μ are the fluid density and viscosity respectively. The geometrical parameters shown in **Fig. 1** R, L, z_b , l_b and t_b are pipe radius, pipe length, blockage location, blockage length and blockage thickness respectively.

B. Dimensionless Analysis

Introducing the following dimensionless variables:

$$r^*=\frac{r}{R},\ z^*=\frac{z}{L},\ v_r^*=\frac{v_r}{U},\ v_z^*=\frac{v_z}{U},\ t^*=\omega t,\ P^*=\frac{P}{\rho U^2}$$

Where; U is a reference velocity and ω is a frequency of oscillation.

Equations (1), (2) and (3) may be written in dimensionless form as follows:

$$S\frac{\partial v_r^*}{\partial t^*}+v_r^*\frac{\partial v_r^*}{\partial r^*}+\frac{R}{L}v_z^*\frac{\partial v_r^*}{\partial z^*}=-\frac{\partial P^*}{\partial r^*}+\frac{1}{Re}\left(\frac{\partial^2 v_r^*}{\partial r^{*2}}+\frac{1}{r^*}\frac{\partial v_r^*}{\partial r^*}-\frac{v_r^*}{r^{*2}}+\frac{R^2}{L^2}\frac{\partial^2 v_r^*}{\partial z^{*2}}\right) \quad (4)$$

$$S\frac{\partial v_z^*}{\partial t^*}+v_r^*\frac{\partial v_z^*}{\partial r^*}+\frac{R}{L}v_z^*\frac{\partial v_z^*}{\partial z^*}=-\frac{R}{L}\frac{\partial P^*}{\partial z^*}+\frac{1}{Re}\left(\frac{\partial^2 v_z^*}{\partial r^{*2}}+\frac{1}{r^*}\frac{\partial v_z^*}{\partial r^*}+\frac{R^2}{L^2}\frac{\partial^2 v_z^*}{\partial z^{*2}}\right) \quad (5)$$

$$\frac{\partial v_r^*}{\partial r^*}+\frac{v_r^*}{r^*}+\frac{R}{L}\frac{\partial v_z^*}{\partial z^*}=0 \quad (6)$$

Where; S is Strouhal Number ($S=\omega R/U$) and Re is Reynolds Number ($Re=\rho UR/\mu$).

International Journal of Engineering Research & Technology (IJERT)
ISSN: 2278-0181
Vol. 5 Issue 06, June-2016

Introducing small perturbation to the main flow and assuming the axial velocity perturbation v^*_{z1} to have the following form:

$$v^*_{z1} = \mathcal{R}[v(r^*, z^*)e^{it^*}] \tag{7}$$

We get:

$$iSv + \frac{R}{L} v^*_{z_o} \frac{\partial v}{\partial z^*} = \frac{1}{Re}\left(\frac{\partial^2 v}{\partial r^{*2}} + \frac{1}{r^*}\frac{\partial v}{\partial r^*}\right) \tag{8}$$

Where; $i=(-1)^{0.5}$ and $\mathcal{R}$ [ ] stands for the real part of oscillations and $v(r^*, z^*)$ is the dimensionless complex velocity amplitude.

Let;

$$v = v_{re} + iv_{im} \tag{9}$$

From (7), (8) and (9) we get;

$$v^*_{z_1} = Y\cos(t^* + \phi) \tag{10}$$

Where; v_{re} is the real part of dimensionless complex velocity amplitude and v_{im} is the imaginary part of dimensionless complex velocity amplitude, $\phi = tan^{-1}(v_{im} / v_{re})$ and $Y=(v^2_{re} + v^2_{im})^{0.5}$, as ϕ is the phase shift angle and Y is dimensionless real velocity amplitude

C. Boundary Conditions

Assuming the boundary conditions for a pipeline with wall surface blockage to be as shown in **Fig.2**, where; $v_{ent}(r^*)$ is the amplitude of velocity disturbance at the entrance of the pipe . t^*_b and l^*_b are the dimensionless blockage thickness and dimensionless blockage length. $v_{ent}(r^*)$ may be assumed to take the form:

$$v_{ent}(r^*) = 0.1\left[sin\left(\pi\left(\frac{r^*}{2} + \frac{1}{2}\right)\right)\right]^{2\gamma} \tag{11}$$

Where; γ is the exponent of velocity disturbance, when γ is increased the disturbance wave becomes thinner around the axis of the pipe and vice versa.

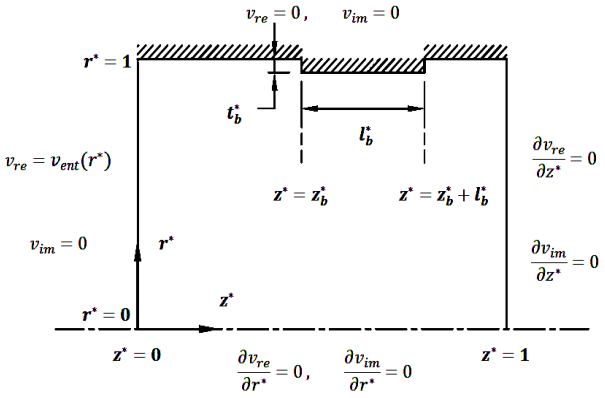

Fig. 2 : Boundary Conditions on the pipe with blockage

D. Wall Shear Stress

The perturbation wall shear stress will be:

$$\tau^*_1|_{r^*=1} = \tau_w \cos(t^* + \beta) \tag{12}$$

Where; $\beta = tan^{-1}(\tau_{im} / \tau_{re})$ and $\tau_w = (\tau^2_{re} + \tau^2_{im})^{0.5}$, as β is a phase shift angle and τ_w is the dimensionless perturbation wall shear stress amplitude.

E. Transformation

The following transformation is used in order to render governing equations well suited to numerical solution:

$$v_{re} = r^{*n} F_{re} \ , \quad v_{im} = r^{*n} F_{im} \tag{13}$$

Where, $n = -0.5$

III. NUMERICAL ANALYSIS

A. Discretization

Discretization is based on the scheme shown in Fig. **3**. The pipe is divided into n-sections in the direction of z^* each section equal to Δz^* and divided into m-sections in the direction of r^* each section equal to Δr^*. As shown Fig. **3** blockage is modeled as reduction in the pipe radius starting at *n1* and ends at *n2* with thickness of blockage *m1*.

Discretized equations using finite difference analysis are:

$$F_{re_{i,j_{New}}} = \xi\left[a_o\left(F_{re_{i-1,j}} - F_{re_{i+1,j}}\right) + a_1\left(F_{re_{i,j+1}} + F_{re_{i,j-1}}\right) + a_2 F_{im_{i,j}}\right] + (1-\xi)F_{re_{i,j_{Old}}} \tag{14}$$

$$F_{im_{i,j_{New}}} = \xi\left[a_o\left(F_{im_{i-1,j}} - F_{im_{i+1,j}}\right) + a_1\left(F_{im_{i,j+1}} + F_{im_{i,j-1}}\right) - a_2 F_{re_{i,j}}\right] + (1-\xi)F_{im_{i,j_{Old}}} \tag{15}$$

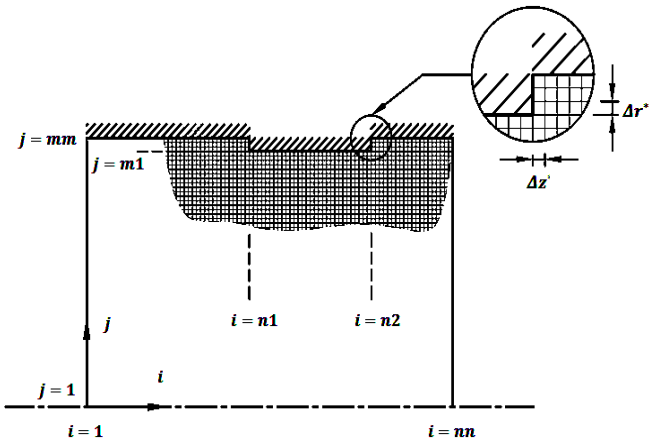

Fig. 3 : Numerical Scheme for pipe with blockage

International Journal of Engineering Research & Technology (IJERT)
ISSN: 2278-0181
Vol. 5 Issue 06, June-2016

Where,

$$a_o = \frac{Re\ C\ v^*_{z_o}}{2\left(\frac{2}{(\Delta r^*)^2}-\frac{1}{4r^{*2}}\right)(\Delta z^*)},\ a_1 = \frac{1}{\left(2-\frac{(\Delta r^*)^2}{4r^{*2}}\right)},\ a_2 = \frac{Re\ S}{\left(\frac{2}{(\Delta r^*)^2}-\frac{1}{4r^{*2}}\right)}$$

And , ξ is the relaxation parameter , C=R/L and v^*_{zo} is the dimensionless steady state axial velocity.

Modified boundary conditions in discretized form as:

$$\left.\begin{array}{ll}
\textbf{\textit{At pipe Entrance }}(i = 1, 1 \le j \le mm); & \\
F_{re_{i,j}} = v_{ent}(r^*)\, r^{*0.5} & ,F_{im_{i,j}} = 0 \\
\textbf{\textit{At pipe Centerline }}(1 < i \le nn, j = 1); & \\
F_{re_{i,j}} = 0 & ,F_{im_{i,j}} = 0 \\
F_{re_{i,j+1}} = \frac{1}{5}\left(4F_{re_{i,j+2}} - F_{re_{i,j+3}}\right) & ,F_{im_{i,j+1}} = \frac{1}{5}\left(4F_{im_{i,j+2}} - F_{im_{i,j+3}}\right) \\
F_{re_{i,j+2}} = \frac{4}{11}F_{re_{i,j+3}} & ,F_{im_{i,j+2}} = \frac{4}{11}F_{im_{i,j+3}} \\
\textbf{\textit{At pipe Exit }}(i = nn, 1 < j < mm); & \\
F_{re_{i,j}} = \frac{1}{3}\left(4F_{re_{i-1,j}} - F_{re_{i-2,j}}\right) & ,F_{im_{i,j}} = \frac{1}{3}\left(4F_{im_{i-1,j}} - F_{im_{i-2,j}}\right) \\
\textbf{\textit{At pipe Surface }}(1 < i \le n1 \text{ and } n2 \le i \le nn, j = mm); & \\
F_{re_{i,j}} = 0 & ,F_{im_{i,j}} = 0 \\
\textbf{\textit{At Blockage }}(n1 \le i \le n2, j = m1) \text{ and} & \\
(m1 < j < mm, i = n1 \,\&\, i = n2); & \\
F_{re_{i,j}} = 0 & ,F_{im_{i,j}} = 0
\end{array}\right\} \quad (16)$$

Discretized wall shear stress will be given as follows:

$$\tau^*_{re_{i,j}} = \frac{1}{Re}\frac{3v^*_{re_{i,j}} + 2v^*_{re_{i,j-2}} - 4v^*_{re_{i,j-1}}}{2(\Delta r^*)} \quad (17)$$

$$\tau^*_{im_{i,j}} = \frac{1}{Re}\frac{3v^*_{im_{i,j}} + 2v^*_{im_{i,j-2}} - 4v^*_{im_{i,j-1}}}{2(\Delta r^*)} \quad (18)$$

B. Algorithm

Successive under relaxation (S.U.R.) method is used for solving the discretized equations Different cases where considered with changes in the length of the blockage and its position along the pipe in order to test the resulting effect of changing blockage length and position on the flow in a pipe. Also the effect of changing *Re*, γ and *S* were tested. Relaxation parameter ξ is varied between 0.1 to 0.2, *C* is fixed at 0.025 for all cases and the relative error is taken to be 0.01.

IV. RESULTS AND DISCUSSION

Fig. 4 to Fig. 6 shows the dimensionless wall shear stress amplitude on the pipe wall and blockage surface along the pipe for three different cases :

- Case 1: Pipe with no blockage
- Case 2: Pipe with blockage starting at a prescribed distance from the pipe entrance say, z^*= 0.24 and extended to the pipe end
- Case 3: Pipe with blockage starting at z^*= 0.24 and extended to say, z^*= 0.64

It is seen that the presence of blockage has a significant effect on the wall shear stress amplitude distribution.

Fig. 4 shows the dimensionless wall shear stress amplitude distribution along the pipe with no blockage (case 1). **Fig. 5** represents the dimensionless wall shear stress amplitude distribution for case 2. It is observed that at z^*= 0.24 there is a sudden drop in τ_w to zero which corresponds to the point on the pipe wall where the blockage begins. At the same station z^* = 0.24 there is a significant rise in the value of τ_w on the blockage surface when compared with value at this point in the no blockage case (case1). The value of τ_w continues to decrease till the end of the pipe.

In **Fig. 6** the value of τ_w drops to zero at z^* = 0.24 and at z^*=0.64 on the pipe wall showing higher value on blockage surface between z^* = 0.24 and z^*= 0.64 when compared with the no blockage case.

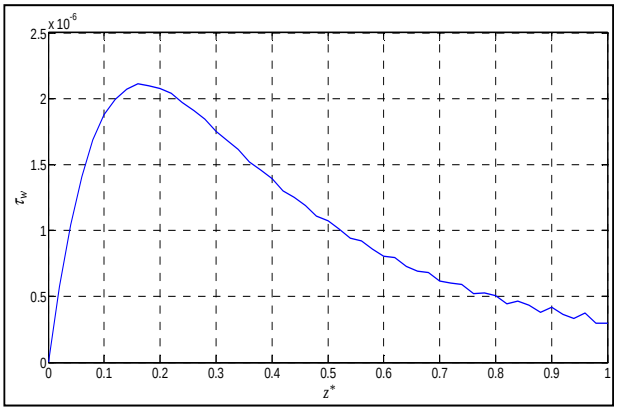

Fig. 4: Dimensionless wall shear stress amplitude distribution [Re=600, S=1, no blockage] – case 1

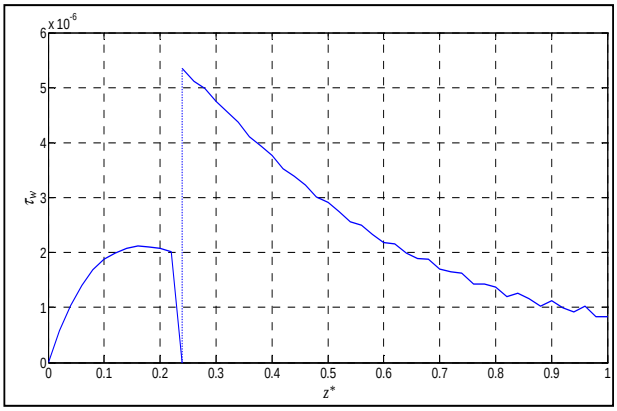

Fig. 5: Dimensionless wall shear stress amplitude distribution [*Re=600, S=1, z^*_b to z^*_l = 0.24 to 1*] – *case 2*

International Journal of Engineering Research & Technology (IJERT)
ISSN: 2278-0181
Vol. 5 Issue 06, June-2016

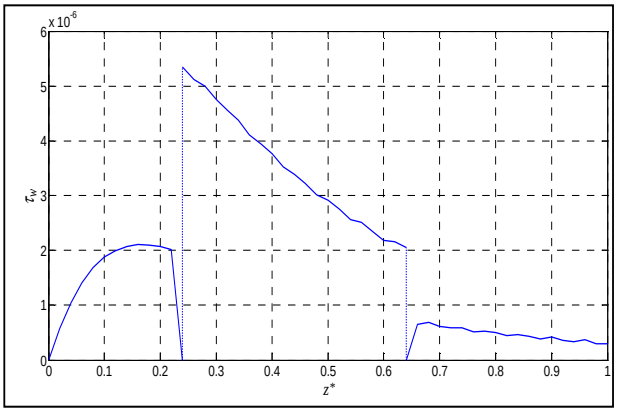

Fig. 6: Dimensionless wall shear stress amplitude distribution [Re=600, S=1, z^*_b to z^*_l = 0.24 to 0.64] - case 3

Where, z^*_b and z^*_l are the dimensionless location of blockage start and blockage end.

In Fig. 7 the difference in τ_w value along the pipe is seen clearly when comparing the three cases. In case 2 , τ_w follows the profile of case 1 in the region before the blockage (z^* = 0 to z^* = 0.22) with a drop of τ_w at the pipe wall and rise in τ_w at blockage surface both of which at z^* = 0.24 . τ_w then continues to decrease till the end of the pipe but still higher than the values of τ_w in the no blockage case (case 1). Similarly for case 3 the value of τ_w follows the profile of case 1 in the region before the blockage (z^* = 0 to z^* = 0.22), a drop in the value of τ_w at z^* = 0.24 at pipe wall takes place followed by a rise in τ_w from z^* = 0.24 to z^* = 0.64 (blockage length) then it drops to zero at z^* = 0.64 and returns back at z^* = 0.66 to follow the same profile of τ_w of the no blockage case (case1). Hence, the wall shear stress amplitude distribution could accurately reflect the location and length of blockage.

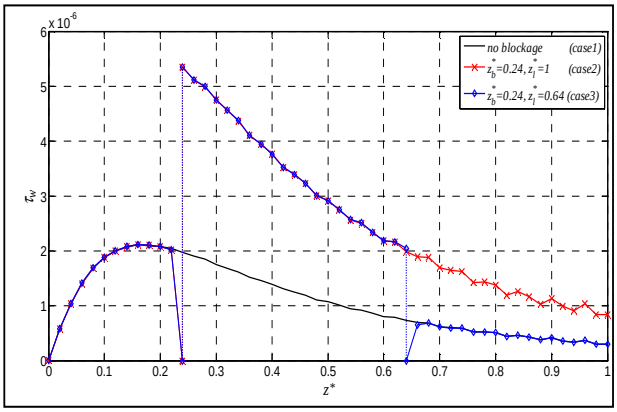

Fig. 7: Dimensionless wall shear stress amplitude distribution [Re=600, S=1] for cases 1, 2 and 3

Fig. 8 illustrates the effect of changing *Re* on the wall shear stress amplitude distribution in a pipe with blockage, for *S=1*, γ=*3* for blockage extending from z^*_b = 0.24 to z^*_l = 0.64 and for *Re = 300,600 and 900*. It is seen that for the same blockage length, τ_w at the pipe wall and blockage surface decreases with the increase of *Re*. It is worth noting here that varying *Re* will affect the value τ_w but doesn't affect the pattern as it remains almost the same. This is illustrated in Fig. **9** which shows the values of τ_w / τ_{wmax} at z^*_b and z^*_l corresponding to *Re =300,600 and 900.*

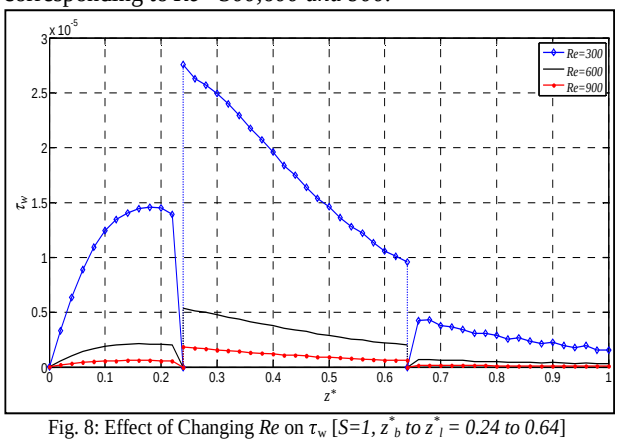

Fig. 8: Effect of Changing *Re* on τ_w [*S=1*, z^*_b *to* z^*_l *= 0.24 to 0.64*]

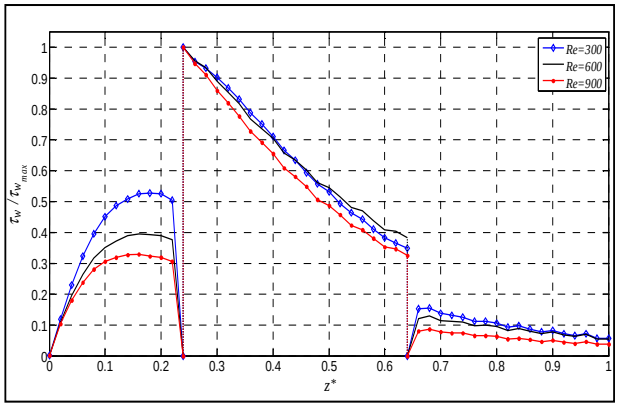

Fig. 9: Effect of Changing *Re* on τ_w / τ_{wmax} [S=*1*, z^*_b *to* z^*_l *= 0.24 to 0.64*]

Fig. 10 shows the effect of changing γ on the distribution of the wall shear stress amplitude in a pipe with blockage, when *Re=600, S=1* for blockage starting at z^*_b = 0.24 to z^*_l=0.64 and for γ=1,3,6 and 9. For the same blockage length increasing γ causes a decrease in τ_w. It is therefore clear that the input signal with γ=1 is recommended to be used as it gives the largest possible response.

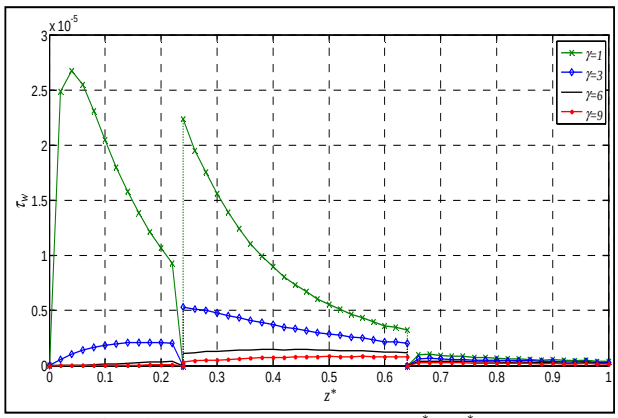

Fig. 10: Effect of changing γ on τ_w [*Re=600, S=1,* z^*_b *to* z^*_l *= 0.24 to 0.64*]

Fig. 11 shows the effect of changing *S* on wall shear stress amplitude distribution in a pipe with blockage, with *Re=600*, γ=1 for blockage starting at z^*_b=0.24 to z^*_l=0.64 and for *S*=0.5,1 and 2. It is observed that for the same blockage

International Journal of Engineering Research & Technology (IJERT)
ISSN: 2278-0181
Vol. 5 Issue 06, June-2016

location and length the value of τ_w on pipe wall and blockage surface decreases with the increase in *S*. This means that lower frequency of the disturbance signal ω will cause higher values of τ_w, which is considered an advantage as the lower frequencies is preferable to be used in practice from the point of view that the pipe structure is not affected and to avoid any damage that could occur to the pipe due to high frequencies and also from the view of measurement as higher frequencies require more sophisticated instruments with higher frequency response.

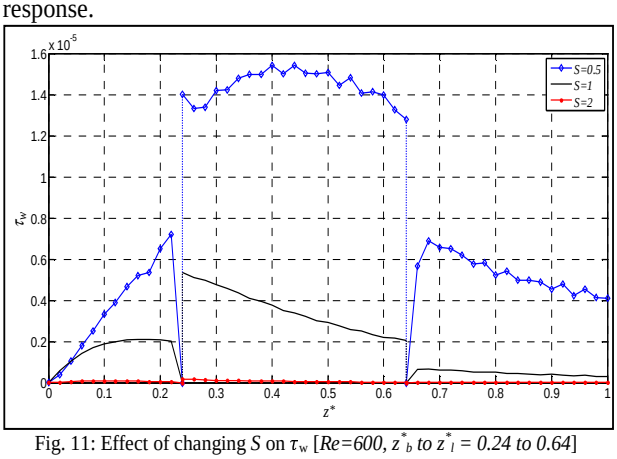

Fig. 11: Effect of changing *S* on τ_w [*Re=600*, z^*_b *to* z^*_l *= 0.24 to 0.64*]

Fig. 12 and Fig. 13 illustrate changes in τ_w due to presence of discrete and extended blockages respectively. Placing one blockage at a time for discrete type at z^*=0.2 and z^*=0.8 and for extended type at z^*=0.1 and z^*=0.6, it is seen that there is a rise in τ_w at the blockage surface each time which reflects the location and the length of the blockage for both cases of discrete and extended types, emphasizing that the blockage location and length could be determined for any type of blockage and at any position in the pipe.

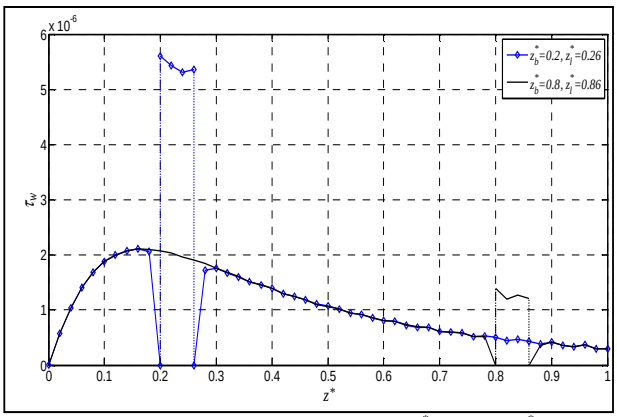

Fig. 12: Comparison for τ_w between blockages at z^*_b *= 0.2* and z^*_l*=0.8 - discrete blockage* [*Re=600, S=1*]

Fig. 14 illustrates changes in τ_w due to presence of different types of blockages that were placed one at a time where all starting at z^*=0.2 and ending at z^*=0.26 for discrete type, z^*=0.5 and 0.8 for extended type. Fig. 15 illustrates changes in τ_w due to presence of extended type blockages that were placed one at a time starting at z^*=0.24,0.5 and 0.74 and all ending at z^*=1. Examining both figures the accuracy of the model is proven to be able to detect the location and length of the blockage irrespective to its extent or its start or end point.

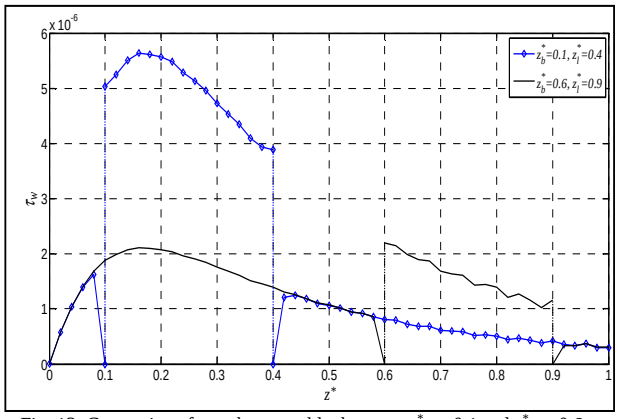

Fig. 13: Comparison for τ_w between blockages at z^*_b *= 0.1* and z^*_b *= 0.6 - extended blockage* [*Re=600, S=1*]

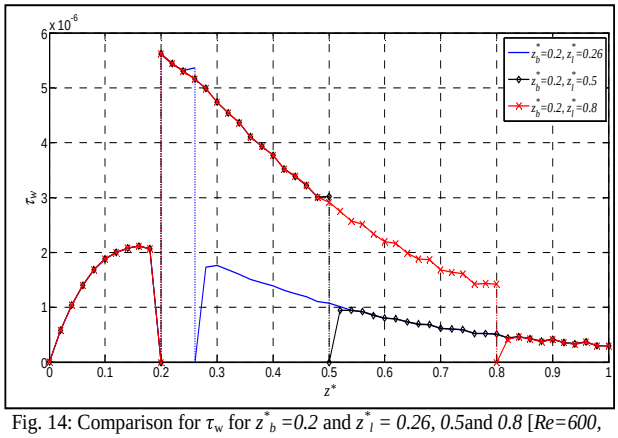

Fig. 14: Comparison for τ_w for z^*_b *=0.2* and z^*_l *= 0.26, 0.5*and *0.8* [*Re=600, S=1*]

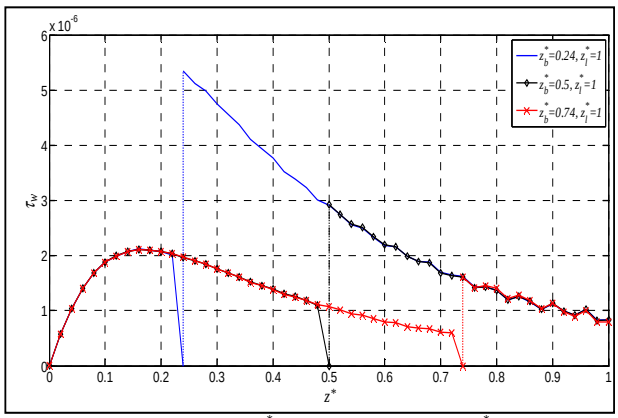

Fig. 15: Comparison for τ_w for z^*_b *=0.24, 0.5* and *0.74* and z^*_l *=1* [*Re=600, S=1*]

V. CONCLUSIONS

The following conclusions are drawn from the foregoing analysis and discussion:

- Presence of blockage causes an increase in the shear stress at the blockage surface
- Lower Reynolds Number will give higher amplitude of shear stress at the blockage surface , changing Reynolds Number does not affect the pattern of wall shear stress distribution along the pipe with blockage

International Journal of Engineering Research & Technology (IJERT)
ISSN: 2278-0181
Vol. 5 Issue 06, June-2016

- Wider disturbance signal is recommended to use as it gives larger response
- Lower Strouhal Number (lower frequency of disturbance) gives higher and more detectable response for the wall shear stress which is an advantage for the proposed technique .
- The proposed model is capable of detecting the location and length of the blockage in a pipe irrespective to its extent or its start or end points with high accuracy.

REFERENCES

[1] H. F. Duan, P. J. Lee, M. S. Ghidaoui and Y. K. Tung, "Extended Blockage Detection in Pipelines by Using the System Frequency Response Analysis," *J. Water Resour. Plann. Manage*, vol. 138, no. 1, pp. 55-62, 2012.

[2] P. J. Lee, J. P. Vitkovsky, M. F. Lambert, A. R. Simpson and J. A. Liggett, "Discrete Blockage Detection in Pipelines Using the Frequency Response Diagram: Numerical Study," *J. Hydraul. Eng.*, vol. 134, no. 5, pp. 658-663, 2008.

[3] E. B. Wylie and V. L. Streeter, Fluid Transients in Systems, New Jersey, USA: Prentice-Hall Inc., Englewood Cliffs , 1993.

[4] M. H. Chaudhry, Applied Hydraulic Transients, 2nd ed., New York, USA: Van Nostrand Reinhold, 1987.

[5] P. K. Mohapatra, M. H. Chaudhry, A. Kassem and J. Moloo, "Detection of Partial Blockages in a Branched Piping System by the Frequency Response Method," *J. Fluids Eng.*, vol. 128, no. 5, pp. 1106-1114, 2006b.

[6] M. A. Adewumi, E. S. Eltohami and W. H. Ahmed, "Pressure Transients Across Constrictions," *J. Energy Resour. Technol.*, vol. 122, no. 1, pp. 34-41, 2000.

[7] M. A. Adewumi, E. S. Eltohami and A. Solaja, "Possible Detection of Multiple Blockages Using Transients," *J. Energy Resour. Technol.*, vol. 125, no. 2, pp. 154-159, 2003.

[8] J. P. Vitkovsky, P. J. Lee, M. L. Stephens, M. F. Lambert, A. R. Simpson and J. A. Liggett, "Leak and Blockage Detection in Pipelines Via an Impulse Response Method," in *5th International Conference Pumps, Electromechanical Devices and Systems Applied to Urban Water Management* , Valencia, Spain, 2003.

[9] X. J. Wang, M. F. Lambert and a. A. R. Simpson., "Detection and Location of a Partial Blockage in a Pipeline Using Damping of Fluid Transients," *J. Water Resour. Plann. Manage.*, vol. 131, no. 3, pp. 244-249, 2005.

[10] P. K. Mohapatra, M. H. Chaudhry, A. A. Kassem and a. J. Moloo, "Detection of Partial Blockage in Single Pipelines," *J. Hydraul. Eng.*, vol. 132, no. 2, pp. 200-206, 2006a.

[11] A. M. Sattar, M. H. Chaudhry and A. A. Kassem, "Partial Blockage Detection in Pipelines by Frequecy Response Method," *J. Hydraul. Eng*, vol. 134, no. 1, pp. 76-89, 2008.

[12] H. F. Duan, P. J. Lee, A. Kashima, J. Lu, M. S. Ghidaoui and Y.-K. Tung, "Extended Blockage Detection in Pipes Using the System Frequency Response: Analytical Analysis and Experimental Verification," *J. Hydraul. Eng.*, vol. 139, no. 7, pp. 763-771, 2013.

[13] S. Meniconi, H. F. Duan, P. J. Lee, B. Brunone, M. S. Ghidaoui and M. Ferrante, "Experimental Investigation of Coupled Frequency and Time-Domain Transient Test–Based Techniques for Partial Blockage Detection in Pipelines," *J. Hydraul. Eng.*, vol. 139, no. 10, pp. 1033-1040, 2013.

[14] M. Stephens, M. Lambert, A. Simpson, J. Vítkovský and J. Nixon, "Field tests for leakage, air pocket, and discrete blockage detection using inverse transient analysis in water distribution pipes," in *Critical transitions in water and environmental resources management : proceedings of the World Water and Environmental Resources Congress*, Salt Lake City, Utah, USA, 2004.

[15] M. L. Stephens, A. R. Simpson and M. F. Lambert, "Hydraulic Transient Analysis and Discrete Blockage Detection On Distribution Pipelines : Field Tests, Model Calibration and Inverse Modelling," in *World Environmental and Water Resources Congress*, Tampa, Florida, USA, 2007.

[16] P. Bocchini, A. Marzani and A. Karamlou, "Blockages Detection in Pipeline Networks for Gas and Oil," in *Shale Energy Engineering Conference 2014*, Pittsburgh, Pennsylvania, USA, 2014.

[17] X. Wang, B. Lennox, G. Short, J. Turner, K. Lewis, Z. Ding, K. Dawson and C. Lewis, "Detecting Blockages and Valve Status in Natural Gas Pipelines," in *Proceedings of 8th International Pipeline Conference*, Calgary, Alberta, Canada, 2010.